

# Adaptation at Synaptic Connections to Layer 2/3 Pyramidal Cells in Rat Visual Cortex

Oliver Beck,<sup>1</sup> Marina Chistiakova,<sup>1,2,3</sup> Klaus Obermayer,<sup>1</sup> and Maxim Volgushev<sup>2,3</sup>

<sup>1</sup>Neural Information Processing Group, Berlin University of Technology, Berlin, Germany; <sup>2</sup>Department of Neurophysiology, Ruhr-University Bochum, Bochum, Germany; and <sup>3</sup>Institute of Higher Nervous Activity and Neurophysiology, Moscow, Russia

Submitted 16 December 2004; accepted in final form 8 March 2005

**Beck, Oliver, Marina Chistiakova, Klaus Obermayer, and Maxim Volgushev.** Adaptation at synaptic connections to layer 2/3 pyramidal cells in rat visual cortex. *J Neurophysiol* 94: 363–376, 2005. First published March 9, 2005; doi:10.1152/jn.01287.2004. Neocortical synapses express differential dynamic properties. When activated at high frequencies, the amplitudes of the subsequent postsynaptic responses may increase or decrease, depending on the stimulation frequency and on the properties of that particular synapse. Changes in the synaptic dynamics can dramatically affect the communication between nerve cells. Motivated by this question, we studied dynamic properties at synapses to layer 2/3 pyramidal cells with intracellular recordings in slices of rat visual cortex. Synaptic responses were evoked by trains of test stimuli, which consisted of 10 pulses at different frequencies (5–40 Hz). Test stimulation was applied either without any adaptation (control) or 2 s after an adaptation stimulus, which consisted of 4 s stimulation of these same synapses at 10, 25, or 40 Hz. The synaptic parameters were then assessed from fitting the data with a model of synaptic dynamics. Our estimates of the synaptic parameters in control, without adaptation are broadly consistent with previous studies. Adaptation led to pronounced changes of synaptic transmission. After adaptation, the amplitude of the response to the first pulse in the test train decreased for several seconds and then recovered back to the control level with a time constant of 2–18 s. Analysis of the data with extended models, which include interaction between different pools of synaptic vesicles, suggests that the decrease of the response amplitude was due to a synergistic action of two factors, decrease of the release probability and depletion of the available transmitter. After a weak (10 Hz) adaptation, the decrease of the response amplitude was accompanied by and correlated with the decrease of the release probability. After a strong adaptation (25 or 40 Hz), the depletion of synaptic resources was the main cause for the reduced response amplitude. Adaptation also led to pronounced changes of the time constants of facilitation and recovery, however, these changes were not uniform in all synapses, and on the population level, the only consistent and significant effect was an acceleration of the recovery after a strong adaptation. Taken together, our results suggest, that apart from decreasing the amplitude of postsynaptic responses, adaptation may produce synapse-specific effects, which could result in a kind of re-distribution of activity within neural networks.

## INTRODUCTION

Brain function depends on synaptic plasticity at several different time scales. At the lower end of the scale ( $\approx 100$  ms) is short-term plasticity, which has been studied in the rat neocortex for synaptic connections formed between different neuron types (Akaneya et al. 2003; Galarreta and Hestrin 1998;

Jia et al. 2004; Markram et al. 1998; Petersen 2002; Reyes et al. 1998; Thomson 1997; Wang and Kaczmarek 1998). The strength of these synaptic connections is changed depending on the activity history of the particular synapse. Mechanisms of the short-term synaptic changes include both release-dependent as well as release-independent components (reviewed in Zucker and Regehr 2002). Simple use-dependent models have been very successfully applied for numerical characterization of the presynaptic component of facilitation and depression at these synapses. It has been shown that models with few degrees of freedom are able to capture essential parts of synaptic dynamics and can in turn be easily interpreted in terms of the depletion of transmitter vesicles after the release and their subsequent replenishment (Abbott et al. 1997; Tsodyks and Markram 1997; Tsodyks et al. 1998; Varela et al. 1997, 1999). The preceding studies characterized the dynamic behavior of synaptic connections after long periods of rest or during low activity levels, that is, essentially without taking into account the history of the high-frequency pre- or post-synaptic activity on the time scale of several seconds. However, it is well known that synaptic dynamics in the neocortex indeed can be altered by a number of manipulations, including induction of long-term plasticity (Markram and Tsodyks 1996; Volgushev et al. 1997) or sensory deprivation (Reyes and Sakmann 1999). On the short time scale of seconds to dozens of seconds, adaptation has been shown to depress responses at the thalamocortical synapses but not at corticocortical synapses of rat somatosensory cortex (Chung et al. 2002). Thus synaptic dynamics can be dramatically influenced by the activity history of that particular synapse on both long- and short-term scales.

The effect of synaptic dynamics on cortical information processing has been investigated in a number of theoretical studies (Adorjan et al. 1999; Artun et al. 1998; Fuhrmann et al. 2002; Goldman et al. 2002). Depression of synaptic transmission in the afferent pathway was suggested as one of the mechanisms contributing to various cortical phenomena, including nonlinear summation, temporal phase shifts, contrast saturation, contrast adaptation or cross-orientation suppression (Carandini et al. 2002; Chance et al. 1998). In particular, it has been proposed that contrast adaptation might be due to a slow form of synaptic depression (Chance et al. 1998) or a slow change in neurotransmitter release probability (Adorjan et al. 1999) at the thalamocortical synapses. Another study (Adorjan et al. 2000) implicated intracortical depression in the optimal coding strategy for the representation of complex stimuli.

Address for reprint requests and other correspondence: O. Beck, Neural Information Processing Group, Berlin University of Technology, 10587 Berlin, Germany (sekr@ni.cs.tu-berlin.de).

The costs of publication of this article were defrayed in part by the payment of page charges. The article must therefore be hereby marked "advertisement" in accordance with 18 U.S.C. Section 1734 solely to indicate this fact.

Motivated by these experimental and theoretical studies we investigated the effect of "adaptation," which consisted of brief, 4-s intervals, of presynaptic activity on the dynamic characteristics of synaptic connections onto rat layer 2/3 pyramidal cells.

## METHODS

The experimental procedures used in this study were in accordance with the guidelines published in the European Communities Council Directive (86/609/EEC 1986) and were approved by the regional animal welfare committee (Arnsberg, Germany).

### Slices

Slices of the visual cortex were prepared as described in detail elsewhere (Volgushev et al. 2004). Wistar rats (P25-P35, Charles River GmbH, Suzfeld, Germany) were anesthetized with ether and decapitated, and the brain was rapidly removed and put into an ice-cold oxygenated solution. Frontal slices of the visual cortex (350- to 400- $\mu\text{m}$  thick) were cut with a vibrotome (Leica, VT 1000S, Nussloch, Germany). After the cutting, the slices were let to recover in an incubator for  $\geq 1$  h at room temperature. The solution used during the preparation of the slices had the same ionic composition as the recording medium (see following text), except for L-glutamine.

### Electrophysiological recordings

For recordings, a slice was put into a submerged chamber. The perfusion medium contained (in mM) 125 NaCl, 2.5 KCl, 2 CaCl<sub>2</sub>, 1.5 MgCl<sub>2</sub>, 1.25 NaH<sub>2</sub>PO<sub>4</sub>, 25 NaHCO<sub>3</sub>, 25 D-glucose, and 0.5 L-glutamine and was aerated with 95% O<sub>2</sub>-5% CO<sub>2</sub> bubbles. All recordings were made at 32–34°C. Patch electrodes were filled with a solution containing (in mM) 127 K-gluconate, 20 KCl, 2 MgCl<sub>2</sub>, 2 Na<sub>2</sub>ATP, 10 HEPES, and 0.1 EGTA and had a resistance of 3–7 M $\Omega$ . Whole cell recordings were made from pyramidal neurons in layers II–III in slices of rat visual cortex. Pyramidal cells were selected under visual control using Nomarski optics and infrared videomicroscopy (Dodt and Zieglgansberger 1990). Reliability of the identification of the

pyramidal cells has been proved in our previous work by labeling the recorded cells with biocytin and morphological reconstruction (Volgushev et al. 2000). Recordings were made with Axoclamp-2A (Axon Instruments) in voltage-clamp mode at holding potential between  $-75$  and  $-85$  mV, which was kept constant for the length of recording from one cell. Synaptic responses were evoked by electric shocks applied through bipolar stimulation electrodes located 0.5–1.5 mm below or lateral to the recording site (Fig. 1). We used low intensity of the stimulation, which was set to produce small postsynaptic responses (excitatory postsynaptic currents, EPSCs) without failures. The electrode signal was digitized at 10 kHz and fed into a computer (PC-486; Digidata 1200 interface and pCLAMP software, Axon Instruments). Data were processed off-line using custom written programs.

### Chemicals

The following chemicals were obtained from Sigma (Deisenhofen, Germany): biocytin, EGTA, HEPES, K-gluconate, L-glutamine, Na<sub>2</sub>ATP. The remaining chemicals were from J. T. Baker B.V., Deventer, Holland.

### Modeling use-dependent synaptic dynamics

To assess parameters of synaptic transmission, we fitted the EPSCs, evoked by repetitive stimulation at different frequencies with a phenomenological model of synaptic transmission (Abbott et al. 1997; Markram et al. 1998; Tsodyks and Markram 1997; Tsodyks et al. 1998). According to the model, a synapse contains a store  $R$  of immediately releasable vesicles, the resource. When an action potential arrives at the presynaptic terminal, it leads to a utilization of a fraction  $U$  of this store, and at the same time, to a temporal increase of the release probability  $U$  by a certain amount. The utilization  $U$  in the model has physiological meaning of release probability. In this manuscript we will use  $U$  in the equations describing the use-dependent model, as in the original account of the model (Tsodyks and Markram 1997), and  $p$  to denote release probability in the binomial release model. The released vesicles are replenished with the time constant  $\tau_{\text{rec}}$ , and release facilitation decays with the time

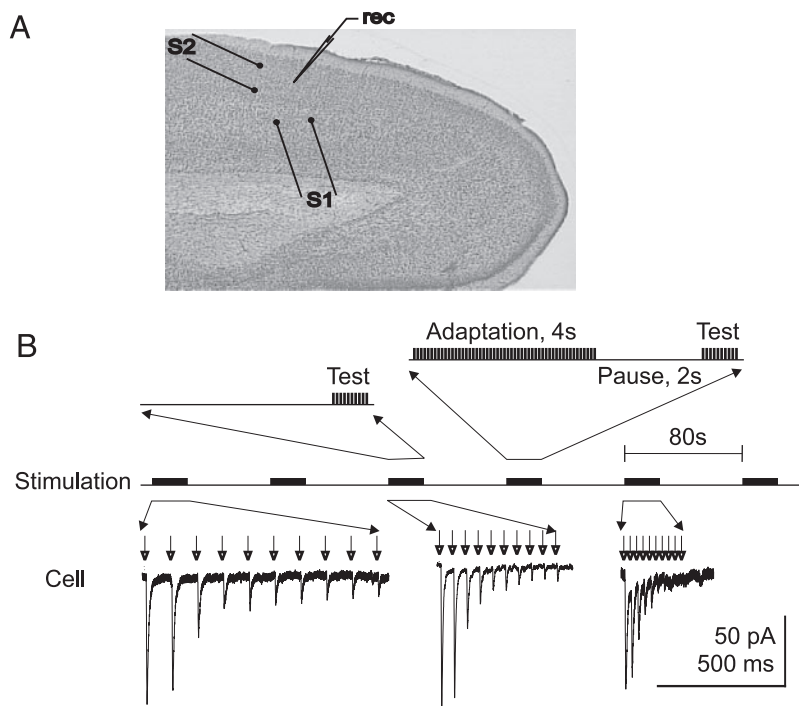


FIG. 1. Recording situation and experimental protocol. *A*: positioning of the stimulation (S1 and S2) and recording electrodes in a slice of the rat visual cortex. *B*: the cartoon illustrates the protocol of stimulation at one of the sites. Stimulation was applied once every 80 s, and consisted of a train of 10 test stimuli at frequencies of 5, 10, 20, or 40 Hz, either preceded by adapting stimulation (expanded on *top right*) or without adaptation (expanded on *top left*). Adapting stimulation consisted of a 4 s train of the stimuli of the same strength, applied at 10, 25, or 40 Hz. After the adaptation, a 2-s interval was set before application of the test stimuli. Stimulation at different frequencies, with or without adaptation was intermingled, as indicated. Test stimulation was applied in alternation at the 2 different stimulation sites.

constant  $\tau_{\text{fac}}$ , both processes are exponential. The released transmitter evokes a current in the postsynaptic neuron that is proportional to the number of released vesicles by a factor  $g$  ( $I = g R U$ ).

Thus our model equations describing the synaptic dynamics are

$$\frac{dR}{dt} = \frac{1-R}{\tau_{\text{rec}}} - UR\delta(t-t_{\text{sp}}) \quad (1)$$

$$\frac{dU}{dt} = \frac{U_0-U}{\tau_{\text{fac}}} + U_0(1-U)\delta(t-t_{\text{sp}}) \quad (2)$$

where  $U_0$  is the utilization of resources  $R$  at very low frequency of stimulation and  $t_{\text{sp}}$  the time of a presynaptic spike. The peak synaptic current is then given by

$$I_{\text{syn}}^{\text{peak}} = gR(t_{\text{sp}})U(t_{\text{sp}}) \quad (3)$$

Equations 1 and 2 can be cast into iterative expressions for  $R$  and  $U$  immediately before the arrival of the  $(n+1)$ -th spike, which depend only on the values for  $R$  and  $U$  immediately before the arrival of the  $n$ -th spike and on the time interval  $\Delta t$  between the  $n$ th and  $(n+1)$ -th spikes

$$R_{n+1} = 1 - \exp(-\Delta t/\tau_{\text{rec}}) + R_n(1-U_n)\exp(-\Delta t/\tau_{\text{rec}}) \quad (4)$$

$$U_{n+1} = U_n(1-U_0)\exp(-\Delta t/\tau_{\text{fac}}) + U_0 \quad (5)$$

When fitting the synaptic responses, we initially assumed that between successive applications of the test stimuli the resources  $R_1$  are fully recovered, that is  $R_1 = 1$ . While this assumption holds for the stimulation without adaptation, as indicated by the stable amplitude of the responses to the first pulses in each train (see RESULTS), it does not hold for the stimuli applied after adaptation.

### Binomial release model

In addition to assessing the release parameters from the response dynamics, we estimated changes in the release probability with the use of quantal analysis (Korn and Faber 1991; Redman 1990; Tarczy-Hornoch et al. 1999). The binomial model of release assumes that all  $n$  release sites contributing to the postsynaptically recorded EPSC have the same release probability  $p$ , release neurotransmitter independently from each other, have the synaptic vesicles of identical size, and, on arrival of an action potential to the presynapse, release either none or exactly one vesicle, which produces a postsynaptic effect of a quantal size  $q$ . The expectation ( $\overline{\text{EPSC}}$ ) and the SD [ $\text{std}(\text{EPSC})$ ] of the evoked EPSC is then given by

$$\overline{\text{EPSC}} = q \cdot np \quad (6)$$

$$\text{std}(\text{EPSC}) = q \cdot [np(1-p)]^{1/2} \quad (7)$$

The coefficient of variation (CV) is

$$\frac{1}{\text{CV}^2} = \frac{np}{1-p} \quad (8)$$

which is independent of the quantal size  $q$  of synaptic vesicles. This in turn leads to the expression

$$p = \frac{1}{\text{CV}^2 n + 1} \quad (9)$$

for the release probability  $p$ , which still depends on the unknown number of release sites  $n$ . Under the reasonable assumption that  $n$  does not change after an adapting stimulus, a change of release probability  $p$  can be estimated. While some of the preceding assumptions are not necessarily always correct, the inverse coefficient of correlation is often considered as one of the indicators of changes of release probability and may be used in combination with other approaches (Faber and Korn 1991; Voronin 1993).

### Stimulus protocol and data analysis

We have assessed parameters of synaptic transmission and their changes after an adaptation by fitting the phenomenological model of synaptic dynamics (Abbott et al. 1997; Tsodyks et al. 1998) to the postsynaptic responses evoked by stimuli at different frequencies. Our experimental protocol is schematically illustrated in Fig. 1. Test stimuli were applied in trains of 10 pulses at 5, 10, 20, or 40 Hz, either after an adapting stimulation or without adaptation. The response of a cell to one train of test stimuli is referred to as one sweep. For adaptation of synapses, we used the same stimuli as in the test trains but applied them for 4 s at 10, 25, or 40 Hz. Thus the higher frequencies led also to the higher number of adapting stimuli. The adaptation was followed by a 2-s interval without stimulation, before a train of test stimuli was applied. In one experiment, we applied test stimuli at three to four different frequencies without adaptation and after an adaptation, either with only one frequency or with one of the two different adapting frequencies. Different combinations of the preceding test and adaptation stimuli were presented intermingled, once in 75–90 s. The stimuli at two stimulation sites (Fig. 1A) were applied in an interleaved manner. Simulations, performed prior to the beginning of electrophysiological recordings, demonstrated that synaptic parameters can be assessed from the responses to three to four test frequencies (data not shown). Therefore for the further analysis we used synaptic connections for which responses to at least five presentations of three different test frequencies, without adaptation and after at least one adapting frequency, were collected. Of 56 synaptic connections, which fulfilled these requirements, 26 could be characterized for two different adaptation frequencies. The amplitudes of EPSCs were measured as the difference between the mean current within two windows of 1- to 5-ms width, one positioned immediately before the response and another one around the peak of the averaged EPSC or on the last portion of the rising slope (Volgushev et al. 2000). For each synaptic connection, the responses obtained with one given set of the adapting and test frequency were averaged and then normalized to the response evoked by the first stimulus in the test train. Our model Eqs. 4 and 5 were then fitted via a least squares method to these normalized responses, obtained with all available test frequencies. Specifically, we were looking for the parameters  $U$ ,  $\tau_{\text{rec}}$ , and  $\tau_{\text{fac}}$  in Eqs. 4 and 5 that led to the best match between model prediction and measured averaged test responses in a least-square sense. As a fitting routine we used a Gauss-Newton method provided by the function `nlinfit` of the statistics toolbox of Matlab (Mathworks, Natick, MA). The maximum number of iterations was set to 500, the termination tolerance for the estimated coefficients as well as the residual sum of squares was chosen as  $10^{-6}$ . The Fig. 2A illustrates the averaged response traces (A1) and normalized EPSC amplitudes together with the best fit for one synaptic connection in the control condition (A2). To estimate the quality of the fits across the sample, we also calculated the root-mean-square (rms) error for each fit. Figure 2B shows the distribution of the rms error per pulse over all synaptic connections in the control (Fig. 2B1) and for all adaptation conditions and control (Fig. 2B2). The mean and median rms error per stimulus for the whole sample were 0.11 and 0.10, respectively, thus a response to a single stimulus could be predicted by the model with an average error of 11%. The rms error is a measure of the quality of the fit, and it shows how well the data are represented by the model. However, it does not by itself say anything about the reliability of the estimation of the free model parameters  $U$ ,  $\tau_{\text{rec}}$ , and  $\tau_{\text{fac}}$  in Eqs. 4 and 5.

To assess this reliability, we have used two approaches. In the first approach, we have performed a series of simulations. For a set of combinations of parameters  $U$ ,  $\tau_{\text{rec}}$ , and  $\tau_{\text{fac}}$ , we simulated the EPSC responses given by Eqs. 4 and 5 and then added to each EPSC a Gaussian noise with a coefficient of variation  $\text{CV} = 0.3$ , which is similar to the values found in the experiments. As in the experiments

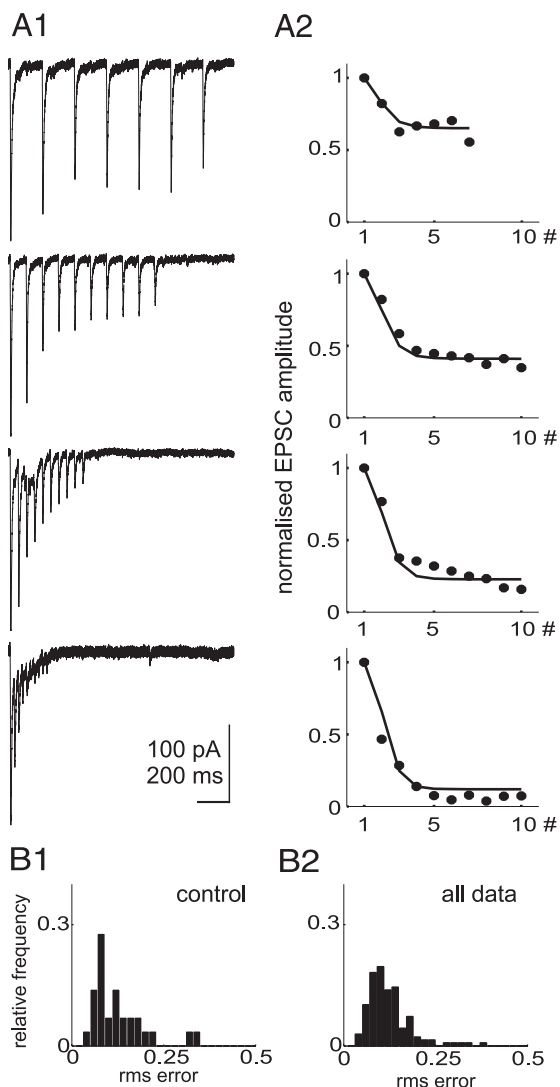


FIG. 2. Synaptic responses evoked by stimulation at different frequencies and results of a fit to the model of synaptic transmission described by Eqs. 4 and 5. *A1*: from top to the bottom: excitatory postsynaptic currents (EPSCs) evoked in a layer 2/3 pyramidal cell in rat visual cortex by the test stimuli applied at 5, 10, 20, and 40 Hz. Each trace is an average of 5 individual responses. *A2*: amplitudes of the EPSCs from *A1*, normalized to the amplitude of the response to the 1st pulse in each train, and plotted against the sequential number of the stimulus in a train (●). —, the optimal fit of responses evoked by all 4 test frequencies. Optimal parameters for this synaptic connection were: release probability,  $U = 0.57$ , facilitation time constant 291.5 ms, recovery time constant 356.2 ms. *B*, 1: distribution of the root-mean-square (rms) error of the fits of control responses (without adaptation), pooled over all 56 synaptic connections; 2: rms error of all fits pooled over all 56 synaptic connections and all available adaptation frequencies ( $n = 138$ ).

we averaged five traces of simulated responses for each test frequency. Then we fitted the optimal parameters  $U$ ,  $\tau_{\text{rec}}$ , and  $\tau_{\text{fac}}$  to these noisy EPSC responses and compared them to the true  $U$ ,  $\tau_{\text{rec}}$ , and  $\tau_{\text{fac}}$  of the noiseless model synapse. The whole procedure was repeated 100 times for each set of synaptic parameters. The results of these simulations showed that estimation of the release probability  $U$  is highly reliable, with a median deviation of  $<7\%$  from the true value of the  $U$ , regardless of the absolute values of the true release probability and facilitation time constant. In addition, the deviation of the estimated  $U$  from the true value decreased rapidly with increasing the recovery time constant used in the simulations. Estimation of the facilitation time constant appeared to be less reliable with a deviation

of  $\leq 30\%$  from the true value in the cases in which a combination of the high true release probability, long facilitation time constant, and short recovery time constant was used. The error in estimation of the facilitation time constant decreased rapidly with increasing the true recovery time constant. Estimation of the recovery time constant showed the strongest dependence on the initial settings used for the simulation of synaptic responses. For the set of true values of the release probability  $U > 0.2$  and recovery time constants shorter than 1.5 s, the deviation of the estimated  $\tau_{\text{rec}}$  from its true value remained  $<15\%$ . With the decreasing values of simulated release probability ( $U < 0.2$ ), the median deviation of the estimated recovery time constant from the true value increased but stayed  $<35\%$ . For the simulated synaptic responses with the combination of low  $U$ , long  $\tau_{\text{rec}}$ , and short  $\tau_{\text{fac}}$ , the estimation of the recovery time constant became unreliable with deviation from the true value increasing to  $>75\%$ . In that latter parameter regime did not only increase the deviation from the true value, but we observed a number of cases with “diverging” ( $>10^3$  s) recovery time constant as the optimal fit to the data. Thus for synapses with a long recovery process ( $\tau_{\text{rec}} > 3\text{--}5$  s) and a low release probability ( $U < 0.2$ ), we frequently (1–25% of all runs) could not attribute a finite recovery process to the synapse based on the optimal root-mean-square fit. Reversing the argument, if our recovery time constant estimate diverged, it was likely that the true recovery time constant was  $>3$  s and the true release probability  $<0.2$ . Because under conditions of our experimental protocol the recovery processes lasting  $>3$  s could not reliably resolved, all “diverging” recovery time constants in the following will be regarded as  $\tau_{\text{rec}} > 3$  s.

In the second approach, we investigated how variable are the estimations of synaptic parameters from repetitive measurements at the same synapse. We therefore increased the number of repetitions of test stimuli and recorded 10–12 sweeps of responses to each test frequency, in the control condition and after an adaptation. For each of the seven synaptic connections recorded with this protocol, we composed 20 random subsets of data, each subset including five randomly chosen sweeps of responses to each test frequency. It should be noted, that different random subsets are not mutually independent, and therefore the following procedure gives only a rough estimate of the true CV of the assessment of synaptic parameters by the model. These random subsets of sweeps were processed as described in the preceding text, and the optimal parameters  $U$ ,  $\tau_{\text{rec}}$ , and  $\tau_{\text{fac}}$  were estimated. The quality of these fits was not different from the rest of the sample, as indicated by the similar values of the mean rms errors (0.11 vs. 0.11 for the rest of the sample). Next, we calculated the CV for the estimated  $U$ ,  $\tau_{\text{rec}}$ , and  $\tau_{\text{fac}}$  for each of the seven synaptic connections. The CV gives an estimate of the reproducibility of the convergence of the model to the same set of optimal synaptic parameter values when different subsets of data from the same synapse are used. The lower the CV, the higher the reproducibility of convergence and thus the reliability of the estimation. The mean CV for the estimated release probability  $U$ , the recovery time constant  $\tau_{\text{rec}}$  and the facilitation time constant  $\tau_{\text{fac}}$  in control were  $\overline{\text{CV}}_U^{\text{NoAdap}} = 0.10$ ,  $\overline{\text{CV}}_{\tau_{\text{rec}}}^{\text{NoAdap}} = 0.13$ , and  $\overline{\text{CV}}_{\tau_{\text{fac}}}^{\text{NoAdap}} = 0.40$ , and after an adaptation the mean CV were  $\overline{\text{CV}}_U^{\text{Adap}} = 0.15$ ,  $\overline{\text{CV}}_{\tau_{\text{rec}}}^{\text{Adap}} = 0.17$ , and  $\overline{\text{CV}}_{\tau_{\text{fac}}}^{\text{Adap}} = 0.46$ .

Taken together, the results of this analysis show that our protocol gives a reliable estimation of the release probability  $U$ , with a low variability of the assessments obtained from the repeated measurements. The recovery time constant  $\tau_{\text{rec}}$  could also be reliably estimated in the above sample, but we expect from our theoretical analysis that this reliability would decrease substantially if the synapses had longer recovery time constants. The estimate of the facilitation time constant is less reliable and varies even between different measurements at the same synaptic connection.

## RESULTS

*Heterogeneity of synaptic properties in control, without previous adaptation*

The dynamic parameters in the control condition without preceding adaptation were highly heterogeneous across the investigated synaptic connections. The distributions of the release probability  $U$ , the recovery time constant  $\tau_{\text{rec}}$ , and the facilitation time constant  $\tau_{\text{fac}}$  over the population of 56 synaptic connections are shown in Fig. 3. The release probability at these synapses varied between 0.04 and 0.57, with predominance of low values (Fig. 3A). The average release probability was  $\bar{U} = 0.21 \pm 0.12$  (median: 0.17). The distribution of the recovery time constant covered a wide range between 85 and  $>3,000$  ms with most of the values  $<1,500$  ms (39 of 56, 70%) but 14 values (25%)  $>3,000$  ms. The facilitation time constant was on average  $\tau_{\text{fac}} = 32.9 \pm 49.7$  ms [median: 14.9 ms; range: 1–278.6 ms]. Altogether, the assessed values of these three synaptic parameters, as well as their large heterogeneity, are in line with previous studies of synaptic characteristics in rat visual cortex (Varela et al. 1997) or somatosensory cortex (Markram et al. 1998). The three synaptic parameters were not independent, but some of them were correlated. A negative correlation has been found between the release probability and the recovery time constant ( $r = -0.47$ ;  $P < 0.0003$ ;  $F$  statistic) and a positive correlation between the release probability and the facilitation time constant ( $r = 0.59$ ;  $P < 2 \cdot 10^{-6}$ ). Thus synapses with higher release probability had shorter recovery time constants and longer facilitation. No significant correlation was found between the facilitation and recovery time constants,  $\tau_{\text{rec}}$  and  $\tau_{\text{fac}}$ .

*Changes in synaptic transmission after adaptation*

Adaptation led to marked changes in synaptic transmission. The most prominent effect, consistently observed after adaptation with any of the three frequencies (10, 25, or 40 Hz) was a reduction of the amplitude of the response to the first stimulus in the test train (EPSC<sub>1</sub>). The synaptic dynamics and assessed parameters of synaptic transmission expressed differential changes after a weak (10 Hz) and strong (25 or 40 Hz) adaptation. In the following text, we will first consider the EPSC<sub>1</sub> amplitude changes and then describe separately changes in synaptic parameters after weak and strong adaptation.

*Decrease of EPSC<sub>1</sub> amplitude after adaptation*

A typical example of the effect of a 10-Hz adaptation on synaptic transmission is illustrated in Fig. 4. The amplitude of

the EPSC<sub>1</sub> decreased after the adaptation to  $\sim 65\%$  of the control value. The EPSC<sub>1</sub> amplitude reduction is clearly seen in the averaged response traces (compare Fig. 4, A1 and B2) and is highly significant ( $P < 2 \cdot 10^{-5}$ ; Wilcoxon nonpaired test). The reduction of the EPSC<sub>1</sub> after adaptation was typical for our sample and occurred in the majority of synaptic connections. In the scatter plot in Fig. 4C, where the amplitude of the EPSC<sub>1</sub> after the 10-Hz adaptation is plotted against the EPSC<sub>1</sub> amplitude in the control condition, most of the points are located below the main diagonal. On average, 10-Hz adaptation led to a reduction of the EPSC<sub>1</sub> amplitude to  $75.5\% \pm 28.3\%$  of the control value (median: 77.3; range: 32.4–164.6%;  $P < 9 \cdot 10^{-5}$ ; Wilcoxon paired test). Stronger adaptation with 25 or 40 Hz led to a yet stronger decrease of the EPSC<sub>1</sub> amplitude (Fig. 5A). After 25-Hz adaptation the first response amplitude dropped to  $65.6\% \pm 23.3\%$  (median: 63.0; range: 32.4–148.2%;  $P < 3 \cdot 10^{-4}$ ) and after a 40-Hz adaptation to  $53.5\%$  (median:  $54.9 \pm 23.5$ ; range: 9.3–93.5%;  $P < 3 \cdot 10^{-6}$ ).

In most of the cases, we recorded synaptic responses in the control condition and after adaptation with one of the three frequencies, therefore the effects of adaptation with different frequencies are compared on the sample basis. To verify the relation between the adaptation strength and the degree of reduction of the EPSC<sub>1</sub> amplitude, we performed control experiments, in which two different adaptation frequencies were used. Data from 26 synaptic connections studied in this way are presented in Fig. 5B. In the scatter plot, the change in the averaged EPSC<sub>1</sub> amplitude after a strong adaptation is plotted against the EPSC<sub>1</sub> amplitude change after a weak adaptation. In all but one connection, the EPSC<sub>1</sub> amplitude decreased more after a strong (25 and 40 Hz, ordinate in Fig. 5B) than after weak (10 Hz, abscissa in Fig. 5B) adaptation. The median difference over the recorded population is  $\text{median}(\Delta\text{EPSC}_1^{40,10}) = \text{median}(\text{EPSC}_1^{40}/\text{EPSC}_1^0 - \text{EPSC}_1^{10}/\text{EPSC}_1^0) = -0.24$  (mean:  $-0.31 \pm 0.25$ ; range:  $-0.89$ – $0.06$ ;  $P < 4 \cdot 10^{-6}$ ; Wilcoxon paired test) for a comparison between 10- and 40-Hz adaptation. Thus at any given synapse, a stronger (higher frequency) adapting stimulation indeed led to a stronger reduction of the EPSC<sub>1</sub> amplitude.

*Recovery of single EPSCs after adaptation*

The decrease of the EPSC<sub>1</sub> amplitude after adaptation was short-lasting and reversible, and the response amplitude recovered to the control value before the next test stimulus was applied (in 75–90 s). To investigate the time course of the recovery of the adaptation-induced decrease of the EPSC<sub>1</sub>, we performed an additional series of experiments, in which seven

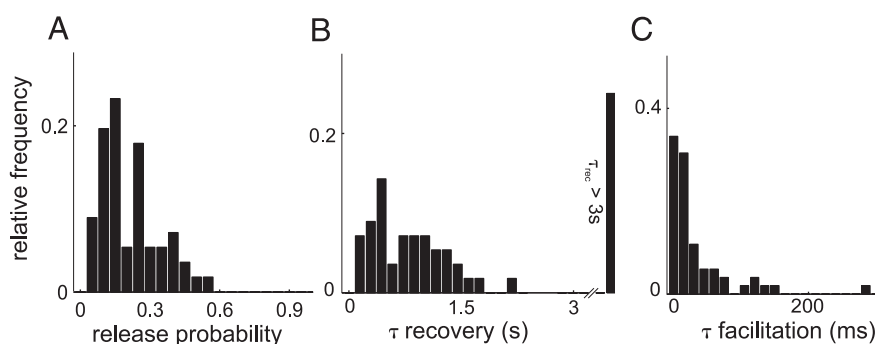


FIG. 3. Distributions of the parameters of best fits of the responses in the control condition, without adaptation. Data for  $n = 56$  synaptic connections. A: release probability  $U$ . B: recovery time constant  $\tau_{\text{rec}}$ . C: facilitation time constant  $\tau_{\text{fac}}$ .

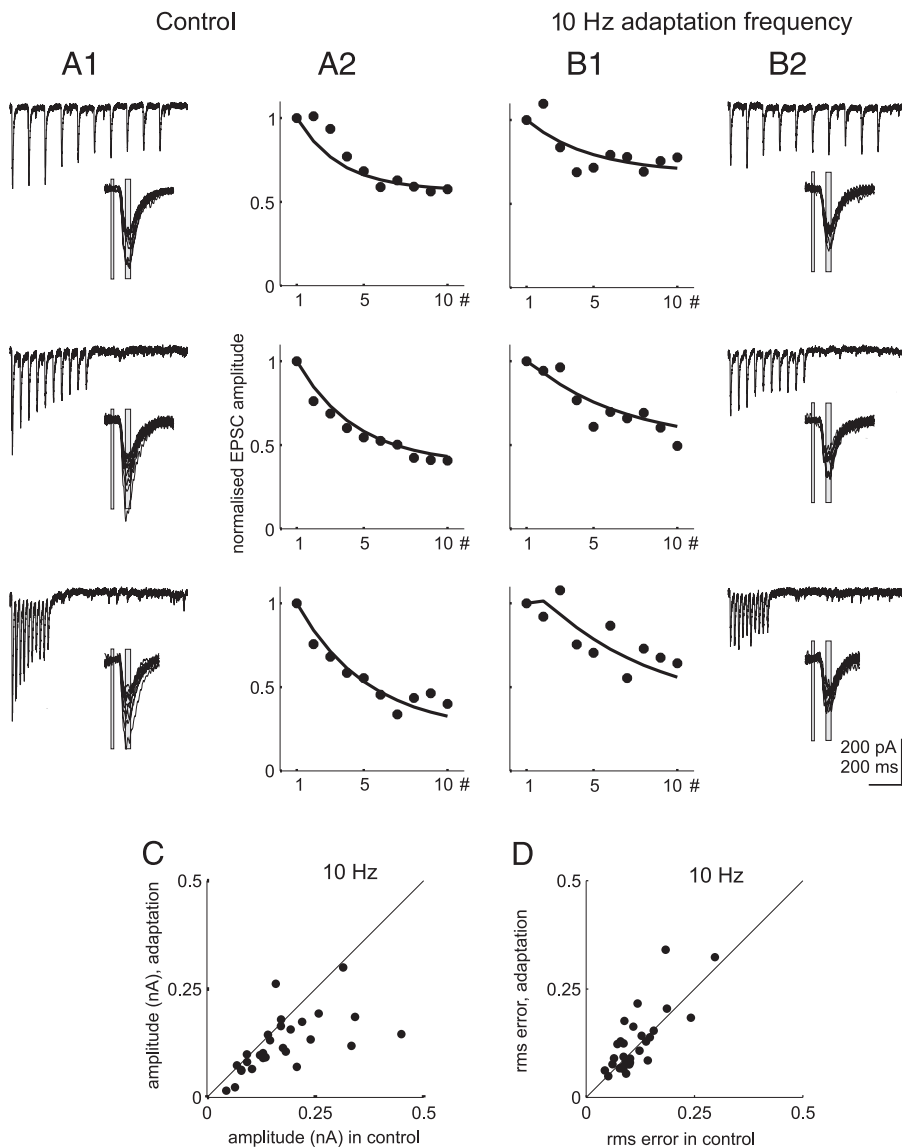


FIG. 4. Synaptic responses and their dynamics in the control condition (A) and after a 10-Hz adaptation (B). A1 and B2: from top to the bottom: EPSCs evoked in a layer 2/3 pyramidal cell in rat visual cortex by test stimuli applied at 10, 20, and 40 Hz. Each trace is an average of 5 individual responses. Insets: superposition of responses to each of the stimuli in the train,  $\square$ , windows for amplitude measurement. A2 and B1: amplitudes of the EPSCs from A1 and B2, normalized to the amplitude of the response to the 1st pulse in each train and plotted against the stimulus number in a train ( $\bullet$ ). —, the optimal fits using Eqs. 4 and 5. Optimal parameters of the fits were: without adaptation (A): release probability,  $U = 0.17$ ; facilitation time constant, 1 ms; recovery time constant, 500.5 ms. After the adaptation (B): release probability,  $U = 0.09$ ; facilitation time constant, 11.7 ms; recovery time constant, 629.9 ms. C: scatter plot showing the relation between the amplitude of responses to the 1st pulse in a train in control (abscissa) and after a 10-Hz adaptation (ordinate). Each point represents data for one synaptic connection ( $n = 29$ ). D: relation between the root mean square (rms) errors of the fits of the responses in the control condition (abscissa) and after a 10-Hz adaptation (ordinate).

test pulses were applied at a low frequency (0.2 Hz) starting 2 s after the end of the adaptation (Fig. 6A1). In the example shown in Fig. 6A, adaptation with 10 Hz lead to only a moderate increase of the response amplitude, but adaptation with 40 Hz led to a marked decrease of the EPSC amplitude (Fig. 6A2). After both, 10- or 40-Hz adaptation, the response amplitude recovered to the control value after 10–20 s. To quantify this recovery process, we fitted a single exponential to the normalized EPSC amplitude responses

$$\text{EPSC}(t) = (\text{EPSC}_0 - \text{EPSC}_\infty) \cdot \exp(-t/\tau) + \text{EPSC}_\infty \quad (10)$$

The three free parameters are the initial EPSC<sub>0</sub> amplitude response that would have been observed immediately after the adaptation stimulus, the control level EPSC<sub>∞</sub> and the time constant  $\tau$  of this recovery process. When fitting the Eq. 10 to the data, the EPSC<sub>0</sub> was constrained to be  $>0$ . Figure 6B shows the relationship between the decrease of the EPSC<sub>1</sub> amplitude after adaptation to 25 or 40 Hz and the optimal fit of the recovery time constant  $\tau$ . The average time constant of the recovery was  $\tau = 7.1 \pm 5.9$  s (median: 5.2 s; range: 1.8–18 s),

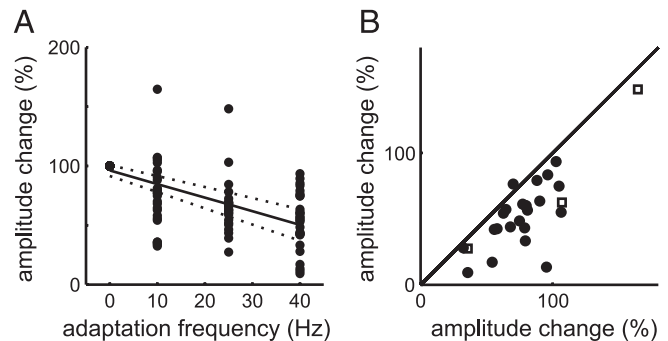


FIG. 5. Changes of the amplitude of the response to the 1st test stimulus in a train after adaptation to different frequencies. A: the EPSC<sub>1</sub> amplitude after an adaptation (ordinate) in percent of the response amplitude in the control conditions, plotted against the frequency of the adapting stimulation (abscissa). — and  $\cdots$ , regression line and 95% confidence intervals. Each point represents data for 1 synaptic connection and 1 adaptation.  $n = 29$  for 10-Hz adaptation,  $n = 24$  for 25-Hz adaptation,  $n = 29$  for 40-Hz adaptation. B: scatter plot of the EPSC<sub>1</sub> amplitude changes after adaptation with 25 Hz ( $\square$ ,  $n = 3$ ) or 40-Hz ( $\bullet$ ,  $n = 23$ ), plotted against the EPSC<sub>1</sub> amplitude change after 10-Hz adaptation at the same synapses (abscissa).

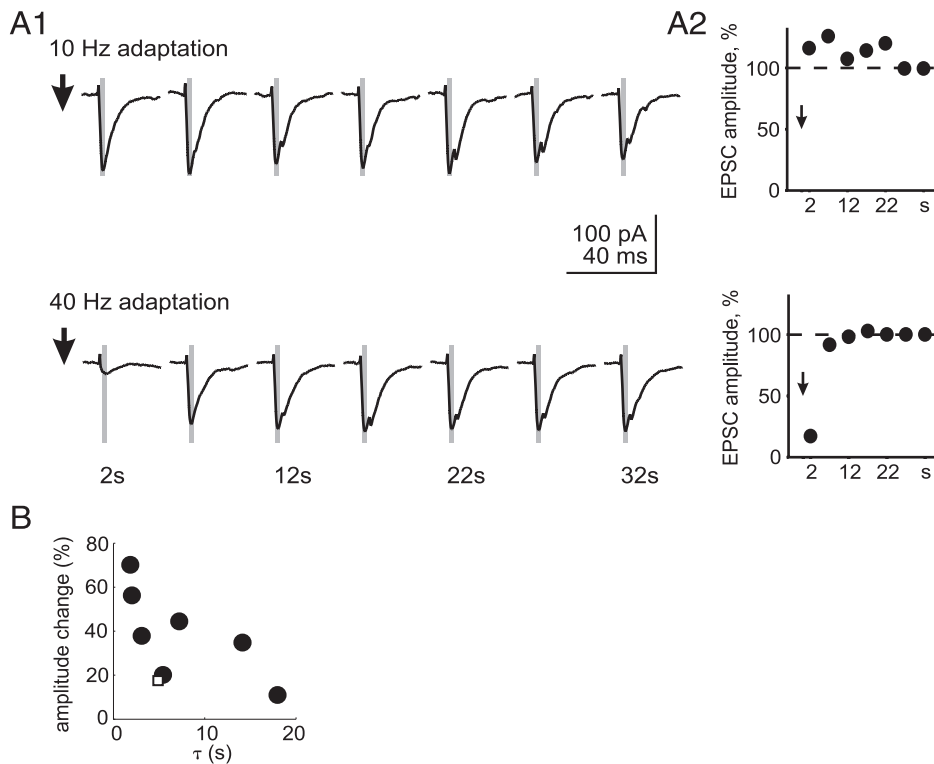


FIG. 6. Recovery of single EPSCs after an adaptation stimulus. *A1*: EPSCs evoked in a layer 2/3 pyramidal cell in rat visual cortex by a stimulus applied at 0.2 Hz starting 2 s after an adaptation stimulus of 10 Hz (*top*) or 40 Hz (*bottom*). Each trace is an average of 10 individual responses. Small positive deflection at the beginning of each response is stimulus artifact.  $\square$ , windows for amplitude measurement. *A2*: amplitudes of the EPSCs from *A1* normalized to the amplitude of the response in the control in percent and plotted against the time after the adaptation.  $\downarrow$ , the time of the end of the adapting train. *B*: the EPSC<sub>1</sub> amplitude after an adaptation with 25 Hz ( $\square$ ) and 40 Hz ( $\bullet$ ) in percent of the response amplitude in the control conditions, plotted against the time constant of an exponential fit to the recovery of EPSC amplitude (abscissa).

the correlation coefficient between the decrease of the EPSC<sub>1</sub> and the time constant  $\tau$  was  $r = -0.6$  ( $P < 0.11$ ;  $F$  statistics).

#### Synaptic changes after weak (10Hz) adaptation

We assessed changes of the synaptic parameters after a weak adaptation with 10-Hz frequency relative to control in 29 synaptic connections. The fitting of control data and of the responses recorded after the adaptation was of comparable, in both cases high, quality. This is illustrated in the scatter in Fig. 4*D*, where the rms errors of the fits of control and adaptation data are plotted against each other. No significant difference was found in the median error between the fits of the responses recorded in control (*median*: 0.09) and after 10-Hz (*median*: 0.10) adaptation ( $P > 0.3$ ; Wilcoxon nonpaired test).

In the example in Fig. 4, the control responses (Fig. 4*A*) were optimally fitted with  $U^0 = 0.17$ ,  $\tau_{\text{rec}}^0 = 500.5$  ms, and  $\tau_{\text{fac}}^0 = 1$  ms. After the adaptation, the best fit was obtained with  $U^{10} = 0.09$ ,  $\tau_{\text{rec}}^{10} = 629.9$  ms, and  $\tau_{\text{fac}}^{10} = 11.7$  ms (Fig. 4*B*). In this example, the decrease in the release probability  $U^{10}/U^0 = 0.53$  can reasonably well account for the reduction of the amplitude of the EPSC<sub>1</sub> (*mean*: 0.64). A decrease of the release probability after a 10-Hz adaptation was typical for our sample as illustrated in Fig. 7*A*, in which for each synaptic connection, the release probability after the adaptation is plotted against the control value. A statistical analysis reveals a highly significant decrease of  $U$  in the population of measured connections [*median*( $\Delta U$ ) = *median*( $U^0 - U^{10}$ ) = 0.030; *mean*:  $0.039 \pm 0.060$ ; *range*:  $-0.05$ – $0.2$ ;  $P < 2 \cdot 10^{-3}$ ; Wilcoxon paired test]. Moreover, the change in the release probability was significantly albeit weakly correlated with the change of EPSC<sub>1</sub> amplitude after the adaptation (Fig. 7*F*, correlation coefficient:  $r = 0.45$ ;  $P < 0.02$ ;  $F$  statistic). These observations, which rely

on the assessment of the release probability from the response dynamics, are corroborated by an independent estimation of the release probability changes with the coefficient of variation method. After the adaptation, the inverse squared coefficient of variation ( $CV^{-2}$ ) of the EPSC<sub>1</sub> amplitude decreased significantly ( $P < 0.04$ ; Wilcoxon paired test), which is indicative of the decreased release probability (Fig. 7*D*). A significant correlation between the change in the  $CV^{-2}$  and the change in the EPSC<sub>1</sub> amplitude ( $r = 0.66$ ;  $P < 1 \cdot 10^{-4}$ ;  $F$  statistic, Fig. 7*E*) lends further support to the conclusion that the reduction of the EPSC<sub>1</sub> amplitude after the adaptation is at least partially due to the decrease of the release probability. However, because the above correlations are weak, and for some synapses changes in EPSC<sub>1</sub> and  $U$  or  $P$  clearly do not go hand in hand, other factors might have contributed to the decrease of the response amplitude after an adaptation. This topic will be elaborated further later in this text.

Other parameters of synaptic transmission, the time constants of recovery,  $\tau_{\text{rec}}$ , and facilitation,  $\tau_{\text{fac}}$ , did not show consistent changes on the population level. It should be noted here that at some synaptic connections the best fit for recovery time constant was out of the range of its reliable estimation. The estimated recovery time constant was  $>3$  s in both, control conditions and after 10-Hz adaptation in four synaptic connections. In three more synapses, the estimated  $\tau_{\text{rec}}$  was  $>3$  s in control, and in five other synapses,  $\tau_{\text{rec}}$  became  $>3$  s after 10-Hz adaptation. All these cases were excluded from the population analysis. For the remaining subpopulation of synaptic connections, in which the estimation of  $\tau_{\text{rec}}$  was reliable ( $\tau_{\text{rec}} < 3$  s) both before and after 10-Hz adaptation (Fig. 7*B*), no significant changes of the recovery time constant were found: *median*( $\Delta \tau_{\text{rec}}$ ) = *median*( $\tau_{\text{rec}}^0 - \tau_{\text{rec}}^{10}$ ) =  $-7.9$  ms; *mean*:  $75.2 \pm 450$  ms; *range*:  $-783$ – $1,092$  ms;  $P > 0.6$ . The facili-

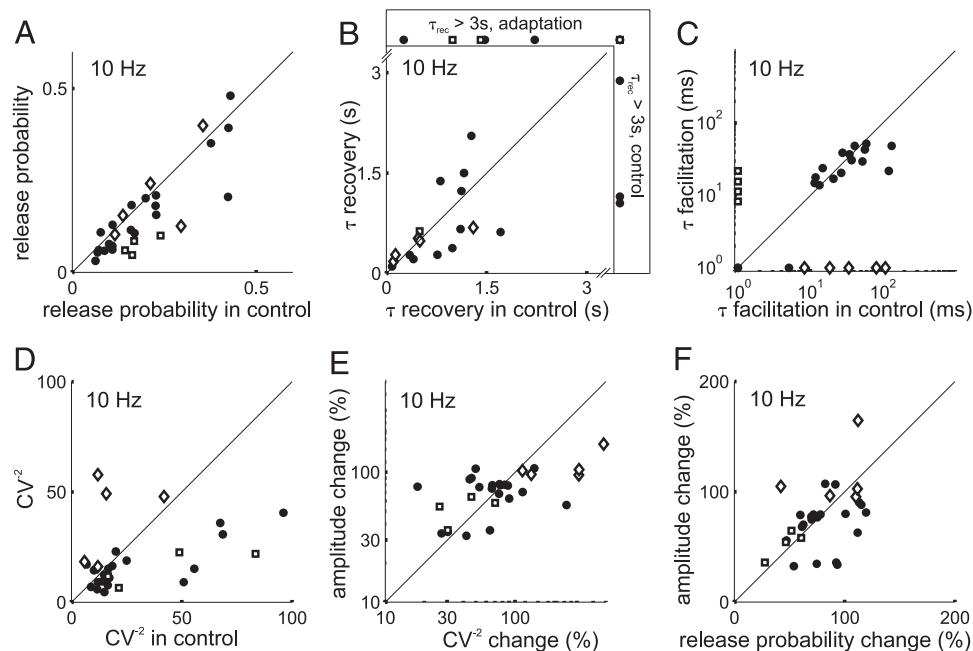


FIG. 7. Change of synaptic parameters after a weak (10 Hz) adaptation. *A–C*: release probability  $U$  (*A*), recovery time constant  $\tau_{\text{rec}}$  (*B*), and facilitation time constant  $\tau_{\text{fac}}$  (*C*), estimated by fitting responses to stimulation with different frequencies (using Eqs. 4 and 5), in the control condition (abscissa) and after 10-Hz adaptation (ordinate). Note the double logarithmic scale in *C* and *E*. *D*: squared inverted coefficient of variation ( $CV^{-2}$ ) of the EPSC<sub>1</sub> amplitude after the 10-Hz adaptation (ordinate) plotted against the  $CV^{-2}$  of the EPSC<sub>1</sub> in the control (abscissa). *E*: change of the amplitude of the EPSC<sub>1</sub> (ordinate) plotted against the change of the  $CV^{-2}$  of the EPSC<sub>1</sub>, in percent of control values. *F*: change of the amplitude of the EPSC<sub>1</sub> (ordinate) plotted against change in the release probability  $U$  (abscissa) in percent of control values. In *A–F*, ●, data for synapses, at which the facilitation time constant after adaptation changed by less than a factor of 6; ◇, for synapses at which facilitation time constant decreased by more than a factor 6; and □, for synapses at which facilitation time constant increased by more than a factor 6.

tation time constant  $\tau_{\text{fac}}$  also did not show significant changes on the population level [Fig. 7*C*, median ( $\Delta\tau_{\text{fac}}$ ) = 0.5 ms; mean:  $13.9 \pm 34.5$  ms; range:  $-21.7$ – $108.3$  ms;  $P > 0.15$ ].

Despite the absence of a unidirectional trend in changes of facilitation and recovery time constants on the population level, individual connections often show a very different behavior before and after the adaptation and alter  $\tau_{\text{rec}}$  and/or  $\tau_{\text{fac}}$  quite dramatically. In Fig. 7, *B* and *C*, in which the values of  $\tau_{\text{rec}}$  and  $\tau_{\text{fac}}$  after the adaptation are plotted against the control values, such cases are represented by points, which are located well away from the main diagonal. Some connections were only weakly depressing in the control but displayed strong depression after an adaptation, or vice versa, as indicated by the increase or decrease of the recovery time constant, respectively. The facilitation time constant expressed most heterogeneous changes, whereby synaptic connections may be subdivided in three distinct groups with respect to the change of facilitation time constant (Fig. 7*C*). In most of the connections, the  $\tau_{\text{fac}}$  changes little (data points around main diagonal in Fig. 7*C*, ●), but in some, it changes from  $\sim 1$  ms, which corresponds to almost purely depressing synapses, to 10–20 ms, making synapses facilitating, or the other way round (data points next to the axes in Fig. 7*C*, ◇, □). To figure out if these groups exhibit special characteristics with regard to other parameters, we have segregated synaptic connections into three groups, one group that increases and one that decreases the facilitation time constant by more than a factor of six and one group in between (Fig. 7*C*, different symbols).

The separation of synaptic connections into these three subgroups neither revealed any group-specific pattern of parameter changes (Fig. 7, *A–F*) nor affected the significance of changes. We then related changes in each synaptic parameter after an adaptation to either changes in other parameters or to their values in the control. From all possible combinations, the only significant correlation was found between the change in release probability  $U$  and the change in the recovery time constant  $\tau_{\text{rec}}$  ( $r = -0.38$ ;  $P < 0.06$ ;  $F$  statistic). Thus a decrease of the release probability after an adaptation was often accompanied by longer recovery of the resources at the presynapse.

#### Synaptic changes after strong (25 or 40 Hz) adaptation

Changes of parameters of synaptic transmission after 25-Hz adaptation were assessed in 24 connections and after 40-Hz adaptation in 29 synaptic connections. The quality of the fits of the responses after 25-Hz adaptation was similar to the quality of fitting the control data (Fig. 8*D1*), and the median rms error in the two data sets showed no significant difference (median: 0.11;  $P > 0.25$ ; Wilcoxon nonpaired test). Fitting of the responses recorded after 40-Hz adaptation was slightly inferior (Fig. 8*D2*) as indicated by a slightly higher median rms error (median: 0.13;  $P < 0.02$ ).

Figures 8, *A* and *B*, illustrate a typical example of synaptic responses in the control and their change after 25-Hz adaptation. Parameters of the optimal fits for this synaptic connection were  $U^0 = 0.27$ ,  $\tau_{\text{rec}}^0 = 839.4$  ms, and  $\tau_{\text{fac}}^0 = 18.6$  ms for the control condition and  $U^{25} = 0.26$ ,  $\tau_{\text{rec}}^{25} = 541.9$  ms, and  $\tau_{\text{fac}}^{25} = 1$

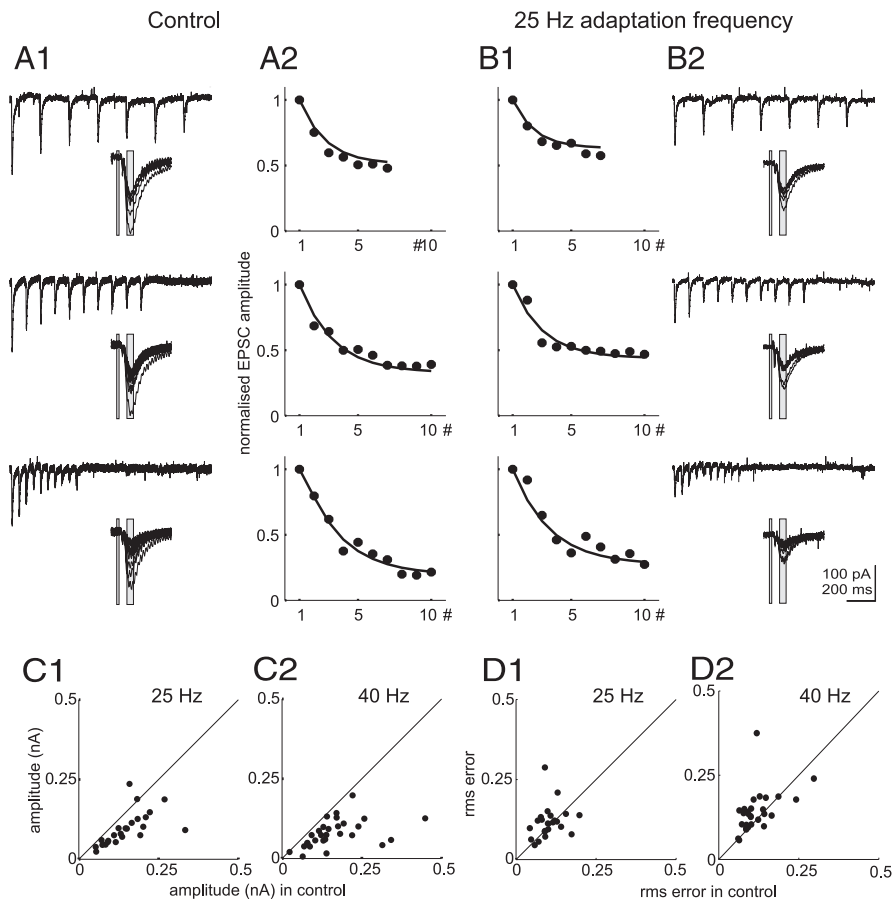


FIG. 8. Synaptic responses and their dynamics in control (A) and after a 25-Hz adaptation (B). A1 and B2: from top to the bottom: EPSCs evoked in a layer 2/3 pyramidal cell in rat visual cortex by the test stimuli applied at 5, 10, and 20 Hz. Each trace is an average of 5 individual responses. Insets: superposition of responses to each of the stimuli in the train;  $\square$ , windows for amplitude measurement. A2 and B1: amplitudes of the EPSCs from A1 and B2, normalized to the amplitude of the response to the 1st pulse in each train and plotted against the stimulus number in a train ( $\bullet$ ). —, the optimal fits according to Eqs. 4 and 5. Optimal parameters of the fits were, without adaptation (A): release probability,  $U = 0.27$ ; facilitation time constant, 18.6 ms; recovery time constant, 839.4 ms. After the adaptation (B): release probability,  $U = 0.26$ ; facilitation time constant, 1 ms; recovery time constant, 541.9 ms. C, 1 and 2: EPSC<sub>1</sub> amplitude after a 25-Hz adaptation (C1,  $n = 23$ , ordinate) and after a 40-Hz adaptation (C2,  $n = 29$ , ordinate), plotted against control values (abscissa). D, 1 and 2: the root mean square (rms) errors of the fits of the responses after a 25-Hz adaptation (D1,  $n = 23$ ) and after a 40-Hz adaptation (D2,  $n = 29$ ), plotted against the rms errors of the fits for the control responses.

ms after a 25-Hz adaptation. The amplitude of the EPSC<sub>1</sub> decreased from 0.15 pA in control to 0.09 pA after an adaptation ( $P < 3 \cdot 10^{-5}$ ).

Thus although the first response amplitude clearly decreased after the adaptation, no accompanying reduction of the release probability was detected by the model. This situation was typical for the effects of strong adaptation with either 25- or 40-Hz stimulation (Fig. 9, A and B). Despite significant decrease of the EPSC<sub>1</sub> amplitude to 66 and 54% of the control, (25- and 40-Hz adaptation, respectively, see preceding text), no significant changes of the release probability over the population were found for either 25- or 40-Hz adaptation [25-Hz adaptation: median( $\Delta U$ ) = median( $U^0 - U^{25}$ ) = 0.004; mean:  $-0.011 \pm 0.055$ ; range:  $-0.122$ – $0.074$ ;  $P > 0.4$ ; 40-Hz adaptation: median:  $-0.029$ ; mean:  $-0.064 \pm 0.197$ ; range:  $-0.764$ – $0.210$ ;  $P > 0.1$ ]. Furthermore, there was no significant correlation between the EPSC<sub>1</sub> amplitude changes and the release probability changes after strong adaptation (Fig. 9, I and J). In contrast to the results of assessment of release probability by fitting response dynamics, the coefficient of variation method indicated a decrease of the release probability after strong adaptation (Fig. 9, G and H). The decrease in the median  $CV^{-2}$  was significant after both 25- and 40-Hz adapting stimuli (25 Hz:  $P < 6.7 \cdot 10^{-4}$ ; 40 Hz:  $P < 3.8 \cdot 10^{-4}$ ; Wilcoxon paired test). Moreover, the changes in the  $CV^{-2}$  and the changes in the EPSC<sub>1</sub> amplitude after strong adaptation were significantly correlated (25 Hz:  $r = 0.58$ ;  $P < 0.003$ ;  $F$  statistic, Fig. 9K; 40 Hz:  $r = 0.39$ ;  $P < 0.03$ , Fig. 9L). When comparing the results of the two methods, however, it is

important to note that the coefficient of variation method relies on stronger assumptions.

Strong adaptation with 25 or 40 Hz led to a significant increase of the rate of recovery of synaptic resources (Fig. 9, C and D). For the subpopulation of synapses, in which the recovery time constant was within the range of reliable estimation ( $\tau_{\text{rec}} < 3$  s) both in the control and after the adaptation, the mean decrease of the recovery time constant after 25-Hz adaptation was  $285.3 \pm 293.3$  ms (median: 333.7 ms; range:  $-256$ – $967$  ms;  $P < 0.003$ ). After an adaptation with 40 Hz, the mean decrease of the recovery time constant was mean ( $\tau_{\text{rec}}^{10} - \tau_{\text{rec}}^{40}$ ) =  $289 \pm 534$  ms (median: 143.6 ms; range:  $-588$ – $1,699$  ms;  $P < 0.008$ ). Those synapses, for which optimal fits were obtained with recovery time constants  $> 3$  s, were excluded from the calculation of the above statistics. However, the higher frequency of occurrence of such synapses in control conditions than after an adaptation (7 in control, 2 after 25-Hz adaptation; 7 in control, 3 after 40-Hz adaptation) also points at shortening of the recovery time after a strong adaptation and thus reinforces the above conclusion.

For the facilitation time constant  $\tau_{\text{fac}}$ , no statistically significant changes on the population level for strong adaptation with either frequency were found (25-Hz adaptation: median: 0 s; mean:  $-33 \pm 201$  ms; range:  $-959.9$ – $109.1$  ms;  $P > 0.6$ ; 40-Hz adaptation: median:  $-14.7$  ms; mean:  $-66.1 \pm 219.7$  ms; range:  $-117.07$ – $39.8$  ms,  $P > 0.05$ ).

Similar to the effects of weak adaptation, we observed three distinct subsets of connections with respect to change of the facilitation time constant. As after the weak adaptation, the

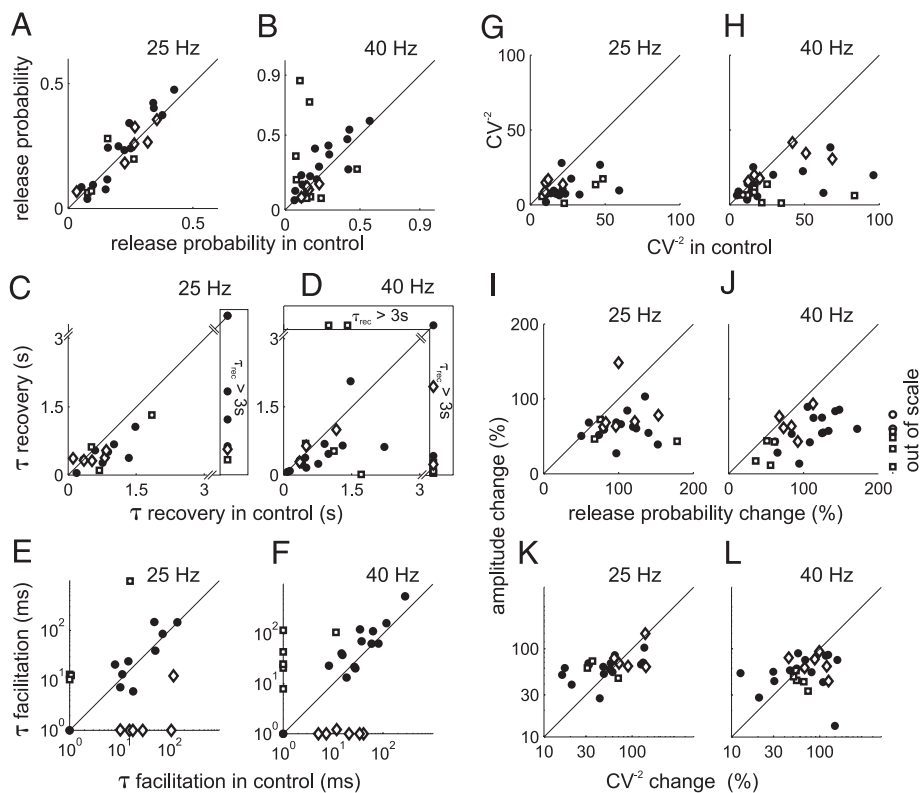


FIG. 9. Change of synaptic parameters after a strong adaptation (25 or 40 Hz). On top of each graph the adaptation frequency is shown. Number of synapses recorded were  $n = 23$  for 25-Hz adaptation,  $n = 29$  for 40-Hz adaptation. In *A–H*, values after adaptation (ordinate) are plotted against control values (abscissa). In *A–L*, data for synapses, at which facilitation time constant after an adaptation changed by less than a factor of 5, are shown as  $\bullet$ , for those with a  $>5$  times decrease of the facilitation time constant as  $\diamond$ , and for synapses with a more than 5x increase of the facilitation time constant as  $\square$ . In *I–L*, changes are given in percent of control. *A* and *B*: release probability. *C* and *D*: recovery time constant. *E* and *F*: facilitation time constant. *G* and *H*: squared inverse coefficient of variation ( $CV^{-2}$ ) of the EPSC<sub>1</sub> amplitude. *I–L*: change of the amplitude of EPSC<sub>1</sub> after an adaptation, plotted against changes of release probability (*I* and *J*) and  $CV^{-2}$  of the EPSC<sub>1</sub> amplitude (*K* and *L*). The out-of-scale values in *J* were: (205.1, 59.8), (384.8, 9.3), (206.2, 79.1), (222.2, 56.6), (817.9, 33.2), (412.3, 48.35).

connections with extreme changes of the facilitation did not express any specific pattern of changes of the other parameters after a strong adaptation, and their omission did not alter the significance of the parameter changes after adaptation. Analysis of the relation between changes of different parameters, reveal the only significant correlation between the change in release probability and the change in the facilitation time constant, which were positively correlated after both 25- and 40-Hz adaptation ( $r = 0.48$ ;  $P < 0.02$  and  $r = 0.72$ ;  $P < 3 \cdot 10^{-5}$ , respectively,  $F$  statistic). This positive correlation is, however, difficult to interpret because neither of these two parameters alone showed significant changes after the strong adaptation. The change in any parameter after strong adaptation stimulus did not correlate significantly with any synaptic parameter in the control state.

To summarize, our analysis revealed the following changes in synaptic transmission after adaptation. 1) Both weak and strong adaptation led to a significant decrease of the EPSC<sub>1</sub> amplitude, the stronger adaptation leading to a stronger decrease of the response amplitude. This decrease was short-lasting, and response amplitude recovered to the control level with a time constant between 2 and 18 s. 2) After weak adaptation, the decrease of the EPSC<sub>1</sub> was accompanied by and correlated with the decrease in release probability, and  $CV^{-2}$ , although some synapses clearly deviated from this rule. 3) After strong adaptation, despite an even stronger reduction of the EPSC<sub>1</sub> amplitude, no change in release probability was revealed from the fits of synaptic dynamics, however, a significant decrease of  $CV^{-2}$  was still observed. 4) Both, weak and strong adaptation had very heterogeneous effects on facilitation and recovery time constants, and thus on the synaptic dynamics. But the only significant change on the population

level was a decrease of the recovery time constant after strong adaptation.

#### Model extension

Inconsistency between the reduction of the EPSC<sub>1</sub> amplitude and the absence of a detected decrease of the release probability after strong adaptation implies that other factors, not accounted for by the simple phenomenological model of synaptic dynamics, were in play. One obvious candidate mechanism here is depletion of the resources, which are not completely recovered after an adaptation. The observed recovery of the depressed EPSC<sub>1</sub> amplitude to the control level with a time constant of several (2–18) seconds corresponds to the suggested time course of refilling of a ready-to-release pool of synaptic vesicles (Sudhof 2000; Zucker and Regehr 2002). To investigate if inclusion of that additional, slow recovery process may influence our estimations of the release parameters, we have extended the original three-parameter model. As a first step, we have included as an additional parameter the amount of resources, available at the beginning of the test train ( $R_1$ )

$$\frac{dR}{dt} = \frac{R_1 - R}{\tau_{rec}} - UR\delta(t - t_{sp}) \quad (11)$$

For fitting the control responses this parameter was set to 1, but for the responses after adaptation, all four parameters ( $R_1$ ,  $U$ ,  $\tau_{fac}$ ,  $\tau_{rec}$ ) were optimized to get the best fit of the data. The best fits of this four-parameter model for  $U$ ,  $\tau_{fac}$ ,  $\tau_{rec}$  did not differ much from the best fits obtained with the original, three-parameter model. Although the four-parameter model did give better fits of the data, as indicated by the decrease of the rms error by 6.9% on the average (median: 5.8%), the optimal values for the release probability, facilitation, and recovery

time constants were not significantly different from the respective values obtained with the three-parameter model. The average differences were, for estimations of the release probability  $U$ , 5.8% (median: 2.1%), for the recovery time constant,  $\tau_{\text{rec}}$ , 1.1% (median: 1.3%), and for the facilitation time constant,  $\tau_{\text{fac}}$ , 15.1% (median: 1.5%).

As the next step, we introduced a second recovery process, which describes slow recovery of the maximal amount of available resources after an adaptation. This maximal amount of resources,  $R^{\text{max}}(t)$  recovers to the limit  $R_{\text{max}}$  with a longer recovery time constant  $\tau_{\text{max}}$ . As initial conditions, we set  $R^{\text{max}}(0) = R_1$  and  $R_{\text{max}} > R_1$ . This extended model is thus described by the following equations

$$\frac{dR}{dt} = \frac{R^{\text{max}}(t) - R}{\tau_{\text{rec}}} - UR\delta(t - t_{\text{sp}}) \quad (12)$$

$$\frac{dR^{\text{max}}}{dt} = \frac{R_{\text{max}} - R^{\text{max}}(t)}{\tau_{\text{max}}} \quad (13)$$

$$\frac{dU}{dt} = \frac{U_0 - U}{\tau_{\text{fac}}} + U_0(1 - U)\delta(t - t_{\text{sp}}) \quad (14)$$

In addition to the free parameters  $U$ ,  $\tau_{\text{rec}}$ , and  $\tau_{\text{fac}}$  from *Eqs. 4* and *5*, three additional parameters  $R_1$ ,  $R_{\text{max}}$ , and  $\tau_{\text{max}}$  have to be estimated in *Eqs. 12–14*. Because fitting all six parameters cannot be done unambiguously, we have fixed the  $\tau_{\text{max}} = 7$  s, which corresponds to the average recovery time constant of the EPSC amplitude after the adaptation, measured experimentally. This extended five-parameter model captured the changes of synaptic responses and their dynamics after both, a weak and a strong adaptation. The results of fitting the responses after the weak adaptation (10 Hz), showed a significant decrease of the release probability, which was correlated with the decrease of the EPSC<sub>1</sub> amplitude ( $r = 0.39$ ,  $P < 0.06$ ,  $F$  statistics). Stronger correlations were found between the decrease of the EPSC<sub>1</sub> amplitude on the one hand, and the decrease of the available resources  $R_1$  ( $r = 0.47$ ,  $P < 0.009$ ) or decrease of the product of  $U$  and  $R_1$  ( $r = 0.99$ ,  $P < 10^{-10}$ ). Interestingly, after the strong adaptation, the extended five-parameter model still did not reveal a change of the release probability, or a correlation between the release probability change and the EPSC<sub>1</sub> amplitude decrease ( $r = -0.07$ ,  $P > 0.6$  for 25-Hz adaptation;  $r = -0.13$ ,  $P > 0.3$  for 40-Hz adaptation). However, the decrease of the EPSC<sub>1</sub> amplitude was significantly correlated with the decrease of estimated resources by the time of application of the first stimulus,  $R_1$  ( $r = 0.70$ ,  $P < 2 \cdot 10^{-4}$  for 25-Hz adaptation and  $r = 0.61$ ,  $P < 6 \cdot 10^{-4}$  for 40-Hz adaptation).

Furthermore, the optimal values for  $U$ ,  $\tau_{\text{fac}}$ ,  $\tau_{\text{rec}}$  estimated with the extended five-parameter model did not differ strongly from the estimations obtained with the three-parameter model. The average differences were, for estimations of the release probability  $U$ , 5.9% (median: 2.1%), for the recovery time constant,  $\tau_{\text{rec}}$ , 2.2% (median: 1.3%), and for the facilitation time constant,  $\tau_{\text{fac}}$ , 15.7% (median: 1.5%). Moreover, inclusion of the second recovery process did not yield superior fits as compared with the four-parameter model.

Taken together, comparison of the assessment of parameters of synaptic transmission and their changes after an adaptation with the help of the original three-parameter model and extended, four- and five-parameter models allows to draw the

following conclusions. First, the estimation of  $U$ ,  $\tau_{\text{fac}}$ , and  $\tau_{\text{rec}}$  is robust because extensions of the model did not lead to notable changes of the estimates of these three basic parameters. Thus the slow recovery of the EPSC<sub>1</sub> after an adaptation did not exert significant influence on estimation of the parameters from responses to brief trains of test stimuli. Second, extended models allowed to quantify the contribution of the resource depletion to the adaptation induced changes of synaptic transmission. Finally, the extended models suggest differential contribution of the changes in release probability and resource depletion to the response changes after adaptation with different frequencies.

## DISCUSSION

The results of our study of the effects of adaptation on synaptic transmission in the visual cortex can be summarized as follows. First, adaptation consistently led to a decrease of the amplitude of the postsynaptic response, stronger adaptation leading to a more pronounced reduction of the response amplitude. This reduction recovered on a time scale of several seconds back to the control level. Second, two possible mechanisms of the response amplitude reduction, decrease of the release probability and decrease of the available resources, were differentially involved in the effects of adaptation with 10, 25, or 40 Hz. Third, adaptation led to heterogeneous changes of dynamics at different synapses, the only consistent and significant effects on the population level being a decrease of the release probability after a weak adaptation and an acceleration of the recovery after a strong adaptation.

### *Estimation of parameters of synaptic transmission in the neocortex*

Before discussing the effects of adaptation on synaptic transmission and dynamics, we shall compare our assessments of the synaptic parameters to the published data. We have recorded small excitatory postsynaptic currents, evoked with the stimulation intensity set just high enough to produce responses without failures. Such weak stimuli, even if recorded in current-clamp mode, evoke postsynaptic responses that are well below the threshold of activation of voltage-gated conductances. Because we have used the same weak intensity of stimulation for both the test trains and the adaptation, we consider as highly unlikely the possibility of contribution of voltage-clamp errors to our results. We have used a modification of a phenomenological model of synaptic transmission (Tsodyks and Markram 1997; Varela et al. 1997) for fitting the synaptic responses, evoked by stimulation with a set of test frequencies. At synaptic connections between layer 5 pyramidal cells in somatosensory cortex, earlier studies reported values for the mean recovery time constants of  $\sim 810$  ms (Markram et al. 1998; Tsodyks and Markram 1997) and 760 ms (Fuhrmann et al. 2004). Applying a modified phenomenological model for the analysis of synaptic connections in rat barrel cortex, Finnerty et al. reported mean recovery time constants of 480–1,190 ms, depending on the group of recorded cells, the developmental history of an animal and experimental conditions (Finnerty and Connors 2000; Finnerty et al. 1999). The preceding results were obtained on synaptic connections involving single axons or few presynaptic fibers.

In a complementary approach, which exploited both intracellularly recorded postsynaptic responses and field potentials, the use of dynamic models for larger populations of synapses has been validated (Varela et al. 1997). Further, the authors demonstrated the usefulness of models of dynamic synapses in prediction of cellular responses to more complex patterns of prolonged stimulation. Varela et al. have found that recovery from the depression could be best described by a bi-exponential process with time constants of several hundreds of milliseconds and several,  $\sim 7$ – $9$ , seconds (Varela et al. 1997). Sparse published data on time constants of facilitation at neocortical synapses show that at synapses between excitatory cells they are usually about a hundred of ms (Markram et al. 1998; Varela et al. 1997), but at synapses, which are formed by pyramidal cells onto interneurons, facilitation of release may last up to several hundreds of milliseconds, making these synaptic contacts highly susceptible for temporal summation (Markram et al. 1998). In the visual cortex synapses in control, we have found recovery time constants in the range of hundreds of milliseconds, with most recovery time constants  $< 1.5$  s, and facilitation time constants in the range from several milliseconds to  $\sim 300$  ms, with the mean of 33 ms. Application of an adapting stimulation revealed an additional, slower recovery process with the time constant of several seconds (mean: 7.1 s). These estimations are in good agreement with the preceding data.

Release probability at neocortical synapses is highly heterogeneous, the values reported so far covering almost the whole possible range. At synapses between layer 5 pyramidal cells in rat somatosensory cortex, possible values of release probability were between 0.025 and 0.9 (Markram et al. 1997). In the barrel cortex, at synaptic connections between layer 4 cells, the release probability was found to be between 0.125 and 0.9 (Feldmeyer et al. 1999). One study reported an exceptionally high release probability, averaged 0.8, at synapses formed by layer 4 stellate cells onto layers 2–3 pyramidal neurons in the barrel cortex (Silver et al. 2003). Our recent study of release probability at synaptic connections to layer 2–3 pyramidal cells in rat visual cortex with the use of MK-801, an open-channel blocker of the *N*-methyl-D-aspartate receptor-gated channels, revealed a skewed distribution of release probabilities, with predominance of values  $< 0.2$  and an average of 0.17 (Volgushev et al. 2004). In the present study, we found similar values of release probability in control, with the average of 0.21 and median of 0.17. Given the high degree of heterogeneity of synaptic connections in the neocortex, where even synapses formed by the same axon onto different postsynaptic cells may express differential dynamic properties (Markram et al. 1998; Reyes et al. 1998; Thomson and Deuchars 1994), these comparisons show that our assessments of parameters of synaptic transmission in control, without adapting stimulation, are in good agreement with the data published so far. Reliability of our estimations of synaptic parameters is further substantiated by the low errors of the fits, which were of comparable range for fits of the data obtained under different conditions of stimulation with and without adaptation and by the fact that an extension of the model by additional parameters did not lead to a notable change of the optimal release probability, facilitation, and depression time constants. Taken together, these results allow us to conclude that our method of estimation of these three basic characteristics of synaptic transmission is reliable

and can be exploited for assessment of changes of synaptic transmission after an adaptation.

#### *Changes of synaptic transmission after adaptation*

In the whole organism, adaptation is expressed as a reduction of the response amplitude. Recent *in vivo* study directly related adaptation of the responses to repetitive sensory stimulation, to the changes of synaptic responses, evoked with electric stimuli (Chung et al. 2002). The authors demonstrated that in rat barrel cortex, adaptation to repetitive whisker stimulation is indeed accompanied by the reduction of the amplitude of the postsynaptic potentials evoked by electric stimulation of the thalamus. Thus the reduction of the response amplitude to repetitive activation of the synapses, either *in vivo* by sensory stimulation, or *in vitro* by applying electric shocks, does serve as a mechanism of adaptation. Our results show that this mechanism might also be involved in adaptation in the visual system, specifically at synapses in the visual cortex, where we have observed reduction of the amplitude of postsynaptic responses after an adapting stimulation. Possible changes of two parameters of the presynaptic release machinery may underlie the reduction of response amplitude after an adaptation: a decrease of the release probability and a decrease of the available synaptic vesicles or resources. Evidence in support of the reduced release probability as one of the reasons for the response amplitude decrease includes the results of our analysis of synaptic dynamics after 10-Hz adaptation, and estimations of the changes of the release probability with the coefficient of variation method. Supportive evidence comes also from the recent somatosensory cortex study in which authors report the decrease of the EPSC amplitude after a train of 20 pulses (Fuhrmann et al. 2004). The authors found that 600 ms after the adapting train, the response amplitude decreased to 43–84% of the control, depending on the adapting frequency and temperature. The decrease of the response amplitude was accompanied by the decrease of the release probability as indicated by the decrease of the inverse coefficient of variation and an increase of the skew of the distribution of response amplitudes (Fuhrmann et al. 2004). The similarity between the results obtained in the visual cortex and in the barrel cortex is further stressed by the similar magnitudes of the response reduction and by the similar dependence of the amplitude reduction on the adaptation strength. In both our data and results of Fuhrmann et al., the depression of responses was stronger after an adaptation with higher frequency. However, we observed a decrease of the release probability in association with the reduction of the response amplitude only after 10-Hz adaptation but not after 25 or 40 Hz, whereas the other study reported a decrease of the release probability after both 10- and 20-Hz adaptation. This apparent inconsistency might well be explained by the different adaptation protocols. We have adapted synapses with 4-s trains at 10, 25, or 40 Hz, whereas Fuhrmann et al. used trains of 20 pulses at 10 or 20 Hz. One possible effect of our adaptation with 25 or 40 Hz for 4 s may be a kind of augmentation, which is typical for synapses in different parts of the brain including the neocortex (e.g., Castro-Alamancos and Connors 1997; Fuhrmann et al. 2004; see Thomson and Deuchars 1994; Zucker and Regehr 2002 for review). The short-term increase of the release probability,

associated with the augmentation, could have counteracted an adaptation-evoked suppression of the release.

One further presynaptic mechanism, which could be responsible for the decrease of the amplitude of postsynaptic responses after an adaptation, is the depletion of a readily releasable pool of synaptic vesicles. During synaptic transmission, the vesicles are released from the immediately releasable pool, which is refilled from the pool of readily releasable vesicles (see Sudhof 2000; Zucker and Regehr 2002 for review). At low rates of presynaptic activity, the size of the larger readily releasable pool does not change substantially, and the recovery is limited by the speed of the vesicle transfer from the readily releasable pool to the immediately releasable pool. This process occurs with a time constant of several hundreds of milliseconds. At high rates of presynaptic activity, the readily releasable pool also becomes depleted and recovery is now limited by the slow process of replenishment (which occurs with a time constant of several seconds) of the readily releasable pool. These two recovery processes are expressed as depression of synaptic transmission with two different, rapid and slow, time courses. Previous studies revealed a slow form of depression, which recovers with a time constant of seconds to tens of seconds also at neocortical synapses (Fuhrmann et al. 2004; Varela et al. 1997). Possible mechanism underlying this form of depression could be the slow replenishment of the readily releasable pool of synaptic vesicles, as suggested by the similarity of the time course of the slowly recovered depression at neocortical synapses, and the replenishment of the readily releasable pool at synapses in other structures (Sudhof 2000; Zucker and Regehr 2002). Our analysis of results with extended models, which took into account this slow recovery process, showed that the relative contribution of the depletion of vesicle pools to the decrease of the response amplitude increases with the adaptation strength. After a weak, 10-Hz adaptation, the reduction of the response amplitude could be accounted for by the reduced release probability with little contribution of the vesicle depletion. In contrast to that, strong adaptation with 25 or 40 Hz led to a significant depletion of the synaptic vesicles, which became the main factor of the response amplitude reduction. Moreover, this analysis demonstrates that the effects of adaptation on synaptic transmission could not be faithfully described by a simple, three-parameter model. Only more complex models, in which interaction between different pools of synaptic vesicles is taken into account, are capable to capture the main features of the response changes after an adaptation. Notably, the time course of the vesicle exchange between different pools is itself a dynamic variable because it can be accelerated by the high-frequency presynaptic firing. This had been demonstrated first for the calyx of Held synapses (Wang and Kaczmarek 1998), and recent study provides evidence for activity dependent acceleration of the vesicle recovery at the synapses in somatosensory cortex (Fuhrmann et al. 2004). Our results on the consistent decrease of the recovery time constant after strong adaptation suggest that a similar acceleration of the vesicle trafficking between different pools might occur also at synapses in the visual cortex. However, further specific experiments are required to clarify the precise time course of these processes at neocortical synapses.

Our study revealed highly heterogeneous changes of dynamic properties of different synaptic connections after an

adaptation. Although adaptation led to changes of the transmission in most of the synapses, the effects vary considerably from one synaptic connection to the other. On the population level, only the decrease of the release probability after a weak adaptation and acceleration of the recovery after a strong adaptation reached significance level. In other cases, synaptic parameters could change even in the opposite directions at different synapses, which resulted in the absence of significant changes in the averaged data. For example, adaptation led to an almost complete disappearance of facilitation at some synapses, but at other synapses, which did not show facilitation in control, it may become apparent after an adaptation. Therefore apart from the decrease of the amplitude of postsynaptic responses, adaptation may produce also cell-specific or synapse-specific effects, which may be averaged out on the population level but could nevertheless result in a kind of redistribution of activity within neural networks. A possible role, which these subtle tunings of network activity may play in sensory adaptation and, more generally in sensory processing, remains to be clarified.

#### ACKNOWLEDGMENTS

We are grateful to P. Balaban for participation in some of the experiments, C. Tacke for technical assistance, and U. Eysel for the support of this project.

#### GRANTS

This work was supported by Deutsche Forschungsgemeinschaft Grant SFB 509 TP A5 to M. Volgushev, SFB 618, and by the BMBF 10025304 Projekt B3 to O. Beck and K. Obermayer.

#### REFERENCES

- Abbott LF, Varela JA, Sen K, and Nelson SB.** Synaptic depression and cortical gain control. *Science* 275: 220–224, 1997.
- Adorjan P, Piepenbrock C, and Obermayer K.** Contrast adaptation and infomax in visual cortical neurons. *Rev Neurosci* 10: 181–200, 1999.
- Adorjan P, Schwabe L, Piepenbrock C, and Obermayer K.** Recurrent cortical competition: Strengthen or weaken? In: *Advances in Neural Information Processing Systems 12*, edited by Müller K.-R. Cambridge, MA: MIT Press, 2000, vol. 12, p. 89–95.
- Akaneya Y, Altinbaev R, Bayazitov IT, Kinoshita S, Voronin LL, and Tsumoto T.** Low-frequency depression of synaptic responses recorded from rat visual cortex. *Neuroscience* 117: 305–320, 2003.
- Artun OB, Shouval HZ, and Cooper LN.** The effect of dynamic synapses on spatiotemporal receptive fields in visual cortex. *Proc Natl Acad Sci USA* 95: 11999–12003, 1998.
- Carandini M, Heeger DJ, and Senn W.** A synaptic explanation of suppression in visual cortex. *J Neurosci* 22: 10053–10065, 2002.
- Castro-Alamancos MA and Connors BW.** Distinct forms of short-term plasticity at excitatory synapses of hippocampus and neocortex. *Proc Natl Acad Sci USA* 94: 4161–4166, 1997.
- Chance FS, Nelson SB, and Abbott LF.** Synaptic depression and the temporal response characteristics of V1 cells. *J Neurosci* 18: 4785–4799, 1998.
- Chung S, Li X, and Nelson SB.** Short-term depression at thalamocortical synapses contributes to rapid adaptation of cortical sensory responses in vivo. *Neuron* 34: 437–446, 2002.
- Doty HU and Zieglgansberger W.** Visualizing unstained neurons in living brain slices by infrared DIC-videomicroscopy. *Brain Res* 537: 333–336, 1990.
- Faber DS and Korn H.** Applicability of the coefficient of variation method for analyzing synaptic plasticity. *Biophys J* 60: 1288–1294, 1991.
- Feldmeyer D, Egger V, Lubke J, and Sakmann B.** Reliable synaptic connections between pairs of excitatory layer 4 neurons within a single “barrel” of developing rat somatosensory cortex. *J Physiol* 521: 169–190, 1999.
- Finnerty GT and Connors BW.** Sensory deprivation without competition yields modest alterations of short-term synaptic dynamics. *Proc Natl Acad Sci USA* 97: 12864–12868, 2000.

- Finnerty GT, Roberts LS, and Connors BW.** Sensory experience modifies the short-term dynamics of neocortical synapses. *Nature* 400: 367–371, 1999.
- Fuhrmann G, Cowan A, Segev I, Tsodyks M, and Stricker C.** Multiple mechanisms govern the dynamics of depression at neocortical synapses of young rats. *J Physiol* 557: 415–438, 2004.
- Fuhrmann G, Segev I, Markram H, and Tsodyks M.** Coding of temporal information by activity-dependent synapses. *J Neurophysiol* 87: 140–148, 2002.
- Galarreta M and Hestrin S.** Frequency-dependent synaptic depression and the balance of excitation and inhibition in the neocortex. *Nat Neurosci* 1: 587–594, 1998.
- Goldman MS, Maldonado P, and Abbott LF.** Redundancy reduction and sustained firing with stochastic depressing synapses. *J Neurosci* 22: 584–591, 2002.
- Jia F, Xie X, and Zhou Y.** Short-term depression of synaptic transmission from rat lateral geniculate nucleus to primary visual cortex in vivo. *Brain Res* 1002: 158–161, 2004.
- Korn H and Faber DS.** Quantal analysis and synaptic efficacy in the CNS. *Trends Neurosci* 14: 439–445, 1991.
- Markram H, Lubke J, Frotscher M, Roth A, and Sakmann B.** Physiology and anatomy of synaptic connections between thick tufted pyramidal neurons in the developing rat neocortex. *J Physiol* 500: 409–440, 1997.
- Markram H and Tsodyks M.** Redistribution of synaptic efficacy between neocortical pyramidal neurons. *Nature* 382: 807–810, 1996.
- Markram H, Wang Y, and Tsodyks M.** Differential signaling via the same axon of neocortical pyramidal neurons. *Proc Natl Acad Sci USA* 95: 5323–5328, 1998.
- Petersen CC.** Short-term dynamics of synaptic transmission within the excitatory neuronal network of rat layer 4 barrel cortex. *J Neurophysiol* 87: 2904–2914, 2002.
- Redman S.** Quantal analysis of synaptic potentials in neurons of the central nervous system. *Physiol Rev* 70: 165–198, 1990.
- Reyes A, Lujan R, Rozov A, Burnashev N, Somogyi P, and Sakmann B.** Target-cell-specific facilitation and depression in neocortical circuits. *Nat Neurosci* 1: 279–285, 1998.
- Reyes A and Sakmann B.** Developmental switch in the short-term modification of unitary EPSPs evoked in layer 2/3 and layer 5 pyramidal neurons of rat neocortex. *J Neurosci* 19: 3827–3835, 1999.
- Silver RA, Lubke J, Sakmann B, and Feldmeyer D.** High-probability unquantal transmission at excitatory synapses in barrel cortex. *Science* 302: 1981–1984, 2003.
- Sudhof TC.** The synaptic vesicle cycle revisited. *Neuron* 28: 317–320, 2000.
- Tarczy-Hornoch K, Martin KA, Stratford KJ, and Jack JJ.** Intracortical excitation of spiny neurons in layer 4 of cat striate cortex in vitro. *Cereb Cortex* 9: 833–843, 1999.
- Thomson AM.** Activity-dependent properties of synaptic transmission at two classes of connections made by rat neocortical pyramidal axons in vitro. *J Physiol* 502: 131–147, 1997.
- Thomson AM and Deuchars J.** Temporal and spatial properties of local circuits in neocortex. *Trends Neurosci* 17: 119–126, 1994.
- Tsodyks M, Pawelzik K, and Markram H.** Neural networks with dynamic synapses. *Neural Comput* 10: 821–835, 1998.
- Tsodyks MV and Markram H.** The neural code between neocortical pyramidal neurons depends on neurotransmitter release probability. *Proc Natl Acad Sci USA* 94: 719–723, 1997.
- Varela J, Sen K, Gibson J, Fost J, Abbott LF, and Nelson S.** A quantitative description of short-term plasticity at excitatory synapses in layer 2/3 of rat primary visual cortex. *J Neurosci* 17: 7926–7940, 1997.
- Varela JA, Song S, Turrigiano GG, and Nelson SB.** Differential depression at excitatory and inhibitory synapses in visual cortex. *J Neurosci* 19: 4293–4304, 1999.
- Volgushev M, Kudryashov I, Chistiakova M, Mukovski M, Niesmann J, and Eysel UT.** Probability of transmitter release at neocortical synapses at different temperatures. *J Neurophysiol* 92: 212–220, 2004.
- Volgushev M, Vidyasagar TR, Chistiakova M, and Eysel UT.** Synaptic transmission in the neocortex during reversible cooling. *Neuroscience* 98: 9–22, 2000.
- Volgushev M, Voronin LL, Chistiakova M, and Singer W.** Relations between long-term synaptic modifications and paired-pulse interactions in the rat neocortex. *Eur J Neurosci* 9: 1656–1665, 1997.
- Voronin LL.** On the quantal analysis of hippocampal long-term potentiation and related phenomena of synaptic plasticity. *Neuroscience* 56: 275–304, 1993.
- Wang LY and Kaczmarek LK.** High-frequency firing helps replenish the readily releasable pool of synaptic vesicles. *Nature* 394: 384–388, 1998.
- Zucker RS and Regehr WG.** Short-term synaptic plasticity. *Annu Rev Physiol* 64: 355–405, 2002.